PROTEIN STRUCTURE REPORT

Structural basis for the negative regulation of bacterial stress response by RseB

Dong Young Kim, Eunju Kwon, JongKeun Choi, Hye-Yeon Hwang, and Kyeong Kyu Kim*

Department of Molecular Cell Biology, Sungkyunkwan University School of Medicine, Suwon 440-746, Korea

Received 29 December 2009; Revised 13 March 2010; Accepted 16 March 2010
DOI: 10.1002/pro.393
Published online 29 March 2010 proteinscience.org

Abstract: The σE-dependent stress response in bacterial cells is initiated by the DegS- and RseP-regulated intramembrane proteolysis of a membrane-spanning antisigma factor, RseA. RseB binds to RseA and inhibits its sequential cleavage, thereby functioning as a negative modulator of this response. In the crystal structure of the periplasmic domain of RseA bound to RseB, the DegS cleavage site of RseA is unstructured, however, its P1 residue is buried in the hydrophobic pocket of RseB, which suggests that RseB binding blocks the access of DegS to the cleavage site.

Keywords: RseA; RseB; RseP; stress response; sigma factor; crystal

Introduction

Regulated intramembrane proteolysis (RIP) is a control mechanism underlying transmembrane signal transfer and performs a key role in the initiation of the essential signal transduction pathways in diverse organisms.[1] For example, the Notch signaling pathway, which is critical for a variety of cell–cell communications in multicellular organisms, is controlled by the RIP of the Notch receptor by ADAM-family metalloprotease and gamma-secretase.[1] In Gram-negative bacteria, the sequential cleavage of RseA, a membrane-spanning anti-σE factor, modulates the initiation of the envelope-stress response.[2,3] RseA forms a tight complex with σE using its N-terminal cytoplasmic domain, thereby inhibiting the transcription of σE-dependent genes. Under stress conditions that include the misfolding of periplasmic proteins, two membrane proteases, DegS and RseP, sequentially degrade RseA to liberate σE (Supporting Information Fig. S1). DegS, which is activated when its PDZ domain is bound to the C-terminal peptide of unfolded outer membrane porins (OMPs), cleaves the C-terminal periplasmic domain of RseA.[4] Subsequently, RseP cleavage within the membrane domain of RseA releases the cytoplasmic domain of RseA (associated with the σE) from the membrane. In the final step, the cytoplasmic domain of RseA is degraded such that the released σE can interact with RNA polymerase.[5] RseB also participates in the regulation of σE-dependent envelope-stress response by inhibiting

Additional Supporting Information may be found in the online version of this article.

Dong Young Kim's current address is Department of Pharmaceutical Chemistry, University of California, San Francisco, 600 16th Street, San Francisco, CA 94107, USA.

Grant sponsor: 21C Frontier Functional Proteomics Program; Grant number: FPR08B2-270; Grant sponsor: Korea Healthcare technology R&D Project; Grant number: A092006; Grant sponsor: Ubiquitome Research Program; Grant number: M105 33010001-05N3301-00100; Grant sponsor: National Research Laboratory Program; Grant number: NRL-2006-02287.

*Correspondence to: Kyeong Kyu Kim, Department of Molecular Cell Biology, Sungkyunkwan University School of Medicine, Suwon 440-746, Korea. E-mail: kkim@med.skku.ac.kr

Table I. *Data Collection and Refinement Statistics*

	$RseA_{peri}$•RseB
Data collection	
Space group	$P2_12_12_1$
Cell dimensions	
a, *b*, *c* (Å)	87.05, 119.58, 150.67
α, β, γ (°)	90.00, 90.00, 90.00
Resolution (Å)	30.00–2.30 (2.38–2.30)[a]
R_{sym} or R_{merge}	6.0 (20.8)
$I/\sigma I$	20.0 (3.5)
Completeness (%)	93.0 (81.5)
Redundancy	4.6
Refinement	
Resolution (Å)	20.00–2.30
No. reflections, working/free	62725/3320
R_{work}/R_{free}	23.9/27.1
No. atoms	
Protein	10108
Zn^{2+}	6
Water	421
B-factors	
Protein	52.1
Zn	82.3
Water	50.0
R.m.s. deviations	
Bond lengths (Å)	0.008
Bond angles (°)	1.482
Ramachandran plot	
Most favored (%)	87.2
Additionally allowed (%)	12.7
Generously allowed (%)	0.2
Disallowed (%)	0.0

[a] Values in parentheses are for highest-resolution shell.

the intramembrane proteolysis of RseA.[6] RseB has been previously demonstrated to suppress the proteolytic activity of DegS for RseA,[6,7] independently of the activation mechanism of DegS.[8] Accordingly, either the deletion of the *rseB* gene or the release of RseB from RseA results in a more rapid degradation of RseA and increased activity of σE.[6,9] In this study, we attempted to characterize the regulatory role of RseB in the proteolytic cleavage of RseA and determined the crystal structure of RseB in complex with $RseA_{peri}$ (the periplasmic domain of RseA, residues 121–216) at a resolution of 2.3 Å by molecular replacement using apo-RseB (PDB ID: 2P4B) as a template (Table I).

Results and Discussion

Structure determination

The $RseA_{peri}$•RseB structure was determined at a resolution of 2.3 Å by molecular replacement using the large domain (residues 26–200) of *E.coli* RseB (PDB ID: 2P4B) as a template.[10] Although the asymmetric unit of the crystal harbors four $RseA_{peri}$•RseB complexes (Supporting Information Fig. S2), the dimeric structure of the complex has been known from size exclusion and SAXS (Small Angle X-ray Scattering) data.[11] Each complex (Com1–Com 4 in Supporting Information Fig. S2) is composed of one RseB monomer and one $RseA_{peri}$ monomer. Com1 is in contact with two other complexes, Com2 and Com3. The Com1:Com2 interaction, which is mediated by hydrogen bonds between relatively well-conserved residues, buries the 1190 $Å^2$ surface area of each complex. RseB:RseB, $RseA_{peri}$:$RseA_{peri}$, and $RseA_{peri}$:RseB interfaces contribute to this burial of surface area by 889 $Å^2$, 57 $Å^2$, and 244 $Å^2$, respectively. The Com1:Com3 interaction results in the burial of 370 $Å^2$, which is primarily a RseB:RseB contact and involves a zinc ion that was added for the purposes of crystallization (Supporting Information Fig. S3). Moreover, the dimeric interaction between the N-terminal regions of the two RseAs in the Com1:Com2 dimer and their proximity to the transmembrane region demonstrate the involvement of the transmembrane domain of RseA in dimeric contacts [Fig. 1(a) and Supporting Information Fig. S4]. There is no biologically relevant higher-order oligomeric form that can be generated by symmetry operations. Accordingly, the Com1:Com2 dimer (or Com3:Com4 dimer) was considered biologically relevant [Fig. 1(a) and Supporting Information Fig. S2]. In this manuscript, we used Com1 and Com1:Com2 to describe the monomeric and dimeric $RseA_{peri}$•RseB complexes, respectively. The RMSD between Com1:Com2 and Com3:Com4 complexes was 0.43 Å for 626 Cα atoms.

Overall structure

We were able to model most residues in RseB, with the exception of the first N-terminal residue, residues 240–246, and three C-terminal residues. The loop connecting the large ($RseB_{25–209}$) and small ($RseB_{217–315}$) domains was disordered in the apo-RseB model[10,12]; however, it was well ordered in the $RseA_{peri}$•RseB complex due to the interaction with the bound $RseA_{peri}$, which results in the stabilization of the loop (Fig. 1). By way of contrast, the 96-residue periplasmic domain of RseA (residues 121–216) was largely unstructured, and only two regions involved in RseB binding, $RseA_{132–151}$ and $RseA_{169–190}$, were modeled (Fig. 1 and Supporting Information Fig. S5). RseB evidenced similar structures in their apo- (Chain A of 2P4B or Chain A of 2V43) and $RseA_{peri}$-bound states, with an RMSD of 0.85 Å for 276 Cα atoms (2P4B) or 1.61 Å for 261 Cα atoms (2V43), thereby indicating that its overall conformation is largely maintained upon RseA binding. The major local conformational change was found in two β-strands (β5 and β6; residues 88–104) in the small domain of RseB (2P4B), which binds directly to the C-terminus of $RseA_{132–151}$ [Fig. 1 and Supporting Information Fig. S6(a)]. The conformational changes are more drastic when the RseA-bound RseB was compared with another crystal structure of apo-RseB (PDB ID: 2V43) where four β-strands (β3–β6; residues 68–104) exhibit large conformational

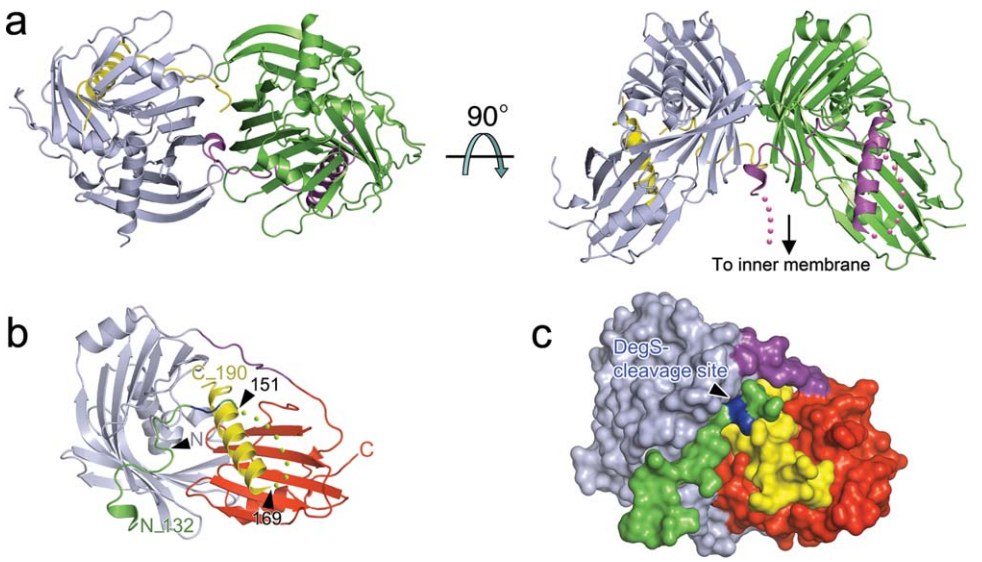

Figure 1. Structure of the $RseA_{peri}$•RseB complex. (a) Dimer model of the $RseA_{peri}$•RseB complex. Each $RseA_{peri}$ is depicted in magenta or yellow, and RseB is depicted in green or slate. Ribbon diagram (b) and surface model (c) of the monomeric $RseA_{peri}$•RseB complex. The regions important for their binding, $RseB_{25–209}$, $RseB_{210–216}$, $RseB_{217–315}$, $RseA_{132–151}$, and $RseA_{169–190}$, are colored slate, purple, red, green, and yellow, respectively. The DegS cleavage site is shown in blue.

changes after binding to the C-terminus of RseA [Fig. 1 and Supporting Information Fig. S6(b)].

Interaction between $RseA_{peri}$ and RseB

RseA binds to a broad area of the RseB groove that is formed between the large and small domains of RseB (Figs. 1 and 2). $RseA_{132–151}$ mostly forms a random coil rather than a regular secondary structure and interacts with residues in the large domain of RseB. The residues in $RseA_{132–151}$ form hydrophobic interactions with the hydrophobic residues or aliphatic carbons of bulky residues of RseB, with the exception of Lys144, which forms a salt-bridge with Glu181 of RseB [Fig. 2(a)]. The results of the histidine pull-down assay verified that an $RseA_{peri}$ mutant featuring Ala substitutions at Gly143, Lys144, and Pro147 was still capable of binding to RseB (data not shown), thereby indicating that the electrostatic interaction attributable to Lys144 is not critically important to the association between RseB and $RseA_{132–151}$. Consistent with this finding, Lys144 is not conserved among RseA homologues in Gram-negative bacteria (Fig. 3).

$RseA_{169–190}$ exhibits a helical conformation and binds principally to the small domain of RseB. The charged residues in $RseA_{169–190}$ are well-conserved in the RseA homologues and are important to RseB binding (Figs. 2 and 3). Most notably, Arg172, Asp179, Glu181, and Arg184/Arg185 in $RseA_{169–190}$ form salt bridges with Glu293, Arg239, Arg282, and Asp109 of RseB, respectively [Figs. 2(a,b)]. It has been demonstrated that $RseA_{169–185}$ is the minimum fragment necessary for RseB binding[8,10]; additionally, the mutation of the conserved Arg residues in this fragment (Arg172, Arg184, and Arg185) abolishes RseB binding activity[10,13] (Fig. 3). Therefore, $RseA_{132–151}$ does not appear to be the primary determinant in RseB binding, but it may perform other additional functions, such as recruiting RseB or sterically inhibiting the access of proteases. Two $RseA_{peri}$•RseB complexes in a dimer (Com1:Com2) are also stabilized via intercomplex interactions [Fig. 1(a) and Supporting Information Fig. S2]. The Val135, Phe136, and Thr138 residues of RseA in Com1 are in contact with Ile50, Asn51/Thr179/Gln182, and Arg169/Arg184 of RseB in Com2, respectively, and vice versa [Figs. 1(a),2(b)].

Structural implication of the binding of RseA to RseB

The DegS cleavage site (Val148-Ser149; P1-P1′) at the C-terminal end of $RseA_{132–151}$, is located within the RseB groove in the $RseA_{peri}$•RseB complex [Figs. 1,2(c)]. Val148 is buried in the hydrophobic pocket formed by Phe100 and Leu102 of RseB and Leu182 of $RseA_{169–190}$. Ser149, which is located near the helix in $RseA_{169–190}$, forms a hydrogen bond with Gln178 of RseA. As a result, the DegS cleavage site is almost completely hidden by RseB and $RseA_{169–190}$, such that DegS access is restricted in the $RseA_{peri}$•RseB complex, and probably also in the RseA•RseB complex (Fig. 1). From this perspective, it has been theorized that the binding of $RseA_{132–151}$ to RseB contributes to locating the cleavage site deep inside of the RseB groove, thereby rendering it resistant to DegS cleavage. This mechanism is consistent with the model proposed in Ref. 8.

In the proteolytic cascade of RseA, the cleavage by RseP requires prior periplasmic cleavage by DegS and the release of $RseA_{149–216}$.[5] It was reported

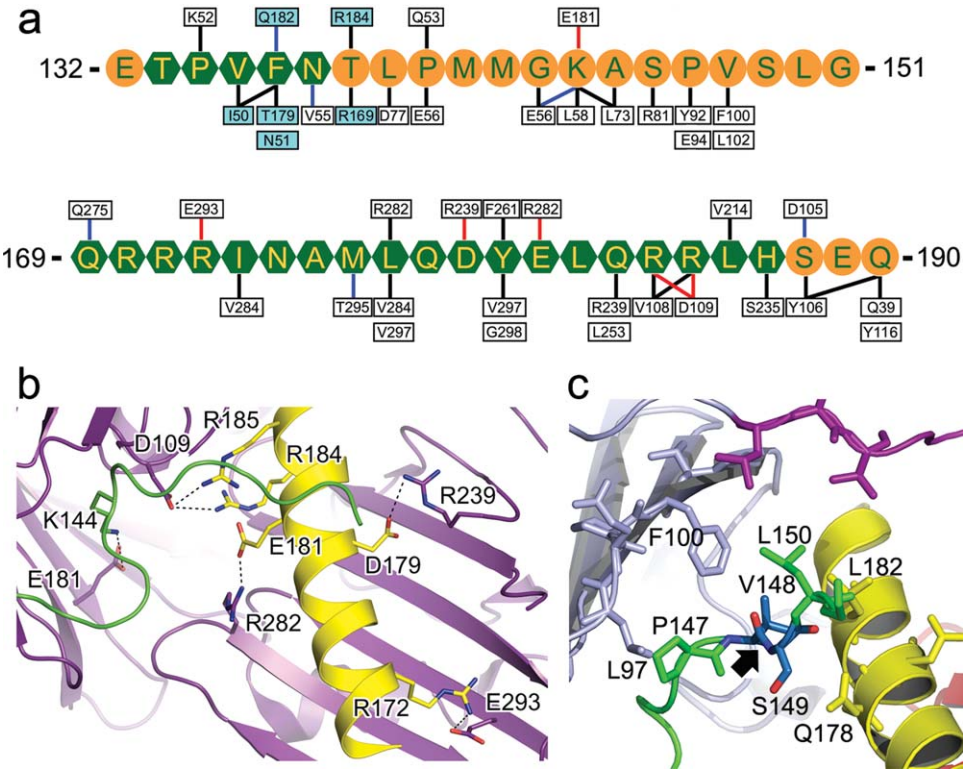

Figure 2. $RseA_{peri}$•RseB interaction. (a) Schematic drawing of $RseA_{peri}$•RseB interaction. RseA residues located in random coils and helices are shown as orange circles and green pentagons, respectively. RseB residues in the same complex and from the other $RseA_{peri}$•RseB complex are marked as white and cyan boxes, respectively. Charge interactions, hydrogen bonds, and hydrophobic contacts are shown as red, blue, and black lines, respectively. (b) Binding interface between RseA and RseB. RseB, $RseA_{132–151}$, and $RseA_{169–190}$ are colored purple, green, and yellow, respectively. Dotted lines indicate charge interactions and the involved residues are depicted by stick models. (c) The DegS cleavage site (Val148-Ser149) bound to the RseB groove in the $RseA_{peri}$•RseB complex is drawn in a ribbon model with the same color scheme as in Fig. 1(b). The residues near the cleavage site are drawn as stick models and labeled. The cleavage site is indicated by a black arrow and labeled.

recently that the interaction of the newly exposed C-terminal residue of $RseA_{1–148}$, Val 148, with the second PDZ domain of RseP is critically important for the cleavage.[14] It is expected that the interaction between RseB and $RseA_{1–148}$ is not very strong due to the lower binding affinity of $RseA_{121–173}$ for RseB detected in previous biochemical studies.[10] These findings suggest that RseB in complex with $RseA_{149–216}$ will dissociate from $RseA_{1–148}$ after DegS cleavage and that RseB is unlikely to

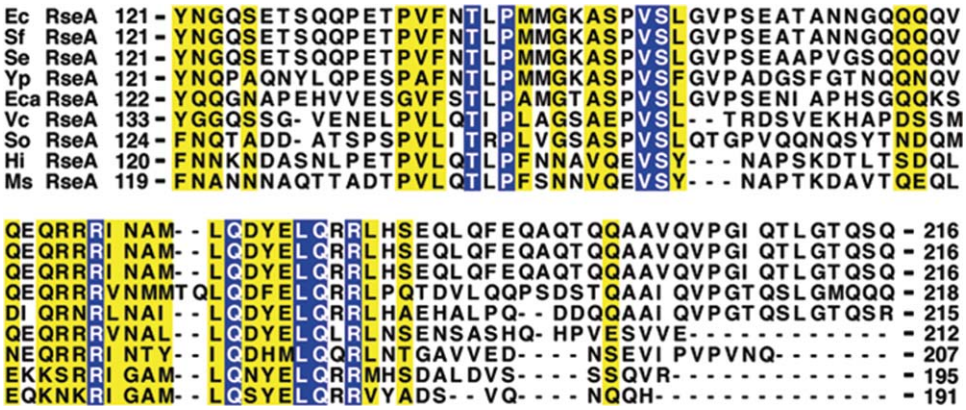

Figure 3. Multiple sequence alignment of the periplasmic domain of RseAs from Gram-negative bacteria. Identical and similar residues are boxed in blue and yellow, respectively. Species abbreviations are as follows: Ec, *Escherichia coli*; Sf, *Shigella flexneri*; Se, *Salmonella enterica*; Yp, *Yersinia pestis*; Eca, *Erwinia carotovora*; Vc, *Vibrio cholerae*; So, *Shewanella oneidensis*; Hi, *Haemophilus influenzae*; Ms, *Mannheimia succiniciproducens*.

reassociate with $RseA_{1–148}$. Therefore, RseP will interact with the C-terminal end of the DegS-cleaved RseA ($RseA_{1–148}$).

Materials and Methods

Protein expression and purification

E.coli $RseA_{peri}$ (periplasmic domain containing residues 121–216) and RseB (residues 24–318) were expressed separately in *E. coli* BL21(DE3) as previously described.[10,11] His-Trx-$RseA_{peri}$- and RseB-expressing cells were harvested and mixed at a ratio of 1:3 (wet weight) to ensure the formation of the complex. The cells were then sonicated in buffer A (20 m*M* Tris-HCl pH 7.5 and 0.1*M* NaCl). The $RseA_{peri}$•RseB complex was then purified by nickel-affinity chromatography and size exclusion chromatography. The cleared lysates were loaded onto a metal-chelating column (GE Healthcare, Princeton, NJ) and the proteins were eluted with 50–500 m*M* imidazole gradient. The fractions containing His-Trx-$RseA_{peri}$•RseB were pooled and dialyzed twice against buffer A. The His-Trx tag was removed with thrombin at room temperature, and $RseA_{peri}$•RseB was purified further using a Superdex-200 column (GE Healthcare, Princeton, NJ) pre-equilibrated with buffer A, then concentrated to 15 mg/mL.

Crystallization and data collection

The crystallization of the $RseA_{peri}$•RseB complex was performed using the microbatch method at 14°C. The crystallization drop was prepared by mixing 1 μL protein solution (8–10 mg/mL) and 1 μL crystallization reagent (28% PEG550MME, 10 m*M* $ZnSO_4$, and 100 m*M* MES pH 6.5) under a layer of Al's oil (Hampton Research, Aliso Viejo, CA). The crystals in a drop were flash-frozen in a cold nitrogen stream at 100 K without the addition of a cryoprotectant, and the diffraction data were collected at PLS-BL4A (Beam line 4A, Pohang Light Source, South Korea; wavelength 1.0000 Å). The diffraction images were recorded to an ADSC Quantum 210 CCD detector. The diffraction data were indexed and integrated using HKL2000 and scaled using SCALEPACK.[15]

Structure determination

The $RseA_{peri}$•RseB structure was determined by molecular replacement using PHASER[16] with the large domain (residues 26–200) of *E.coli* RseB[10] (PDB 2P4B) as a template. Three large domains were initially identified, and the small domains were added to the model. The fourth RseB was generated by a noncrystallographic symmetry operation. Several cycles of rigid body, positional, simulated annealing and B-factor refinements, and model rebuilding were conducted at a resolution of 2.3 Å using the CNS and COOT programs.[17,18] The RseA model was placed on the additional electron density. The $RseA_{peri}$•RseB structure was refined further using REFMAC.[19] The final refinement with solvents resulted in R and R_{free} values of 23.8% and 27.0%, respectively. The data collection and refinement statistics are summarized in Table I. The figures were drawn using PyMOL.[20] The protein–protein interface was calculated using Protorp.[21] The coordinates and structure factors for the $RseA_{peri}$•RseB complex have been deposited under accession code 3M4W.

Summary

In this study, we characterized the inhibitory mechanisms of RseB in the regulated proteolysis of RseA. The C-terminal helix in $RseA_{169–190}$ is a major contributor to the formation of a stable complex with RseB, whereas the N-terminal region of the periplasmic domain of RseA is necessary for the burial of the DegS cleavage site within an inaccessible pocket in the RseA•RseB complex. In the regulation of the envelope-stress response, RseB functions by blocking the access of DegS protease rather than converting RseA into a compact structure that is resistant to proteolysis, as the random coil structure around the cleavage site is maintained in the complex. Accordingly, in this study we explain why the release of RseB is a prerequisite for the degradation of RseA and the activation of the σE-dependent envelope stress response at the atomic level. In the crystal structure of the RseA•RseB complex, RseB is unlikely to interfere with the further degradation of the periplasmically cleaved RseA. Therefore, the newly exposed Val148 will be readily recognized by RseP for subsequent cleavage, which results in the activation of the envelope-stress response.

References

1. Brown MS, Ye J, Rawson RB, Goldstein JL (2000) Regulated intramembrane proteolysis: a control mechanism conserved from bacteria to humans. Cell 100: 391–398.
2. Alba BM, Leeds JA, Onufryk C, Lu CZ, Gross CA (2002) DegS and YaeL participate sequentially in the cleavage of RseA to activate the sigma(E)-dependent extracytoplasmic stress response. Genes Dev 16:2156–2168.
3. Kanehara K, Ito K, Akiyama Y (2002) YaeL (EcfE) activates the sigma(E) pathway of stress response through a site-2 cleavage of anti-sigma(E), RseA. Genes Dev 16: 2147–2155.
4. Walsh NP, Alba BM, Bose B, Gross CA, Sauer RT (2003) OMP peptide signals initiate the envelope-stress response by activating DegS protease via relief of inhibition mediated by its PDZ domain. Cell 113:61–71.
5. Flynn JM, Levchenko I, Sauer RT, Baker TA (2004) Modulating substrate choice: the SspB adaptor delivers a regulator of the extracytoplasmic-stress response to the AAA+ protease ClpXP for degradation. Genes Dev 18:2292–2301.
6. Grigorova IL, Chaba R, Zhong HJ, Alba BM, Rhodius V, Herman C, Gross CA (2004) Fine-tuning of the

Escherichia coli sigmaE envelope stress response relies on multiple mechanisms to inhibit signal-independent proteolysis of the transmembrane anti-sigma factor, RseA. Genes Dev 18:2686–2697.
7. Chaba R, Grigorova IL, Flynn JM, Baker TA, Gross CA (2007) Design principles of the proteolytic cascade governing the sigmaE-mediated envelope stress response in *Escherichia coli*: keys to graded, buffered, and rapid signal transduction. Genes Dev 21:124–136.
8. Cezairliyan BO, Sauer RT (2007) Inhibition of regulated proteolysis by RseB. Proc Natl Acad Sci USA 104: 3771–3776.
9. Collinet B, Yuzawa H, Chen T, Herrera C, Missiakas D (2000) RseB binding to the periplasmic domain of RseA modulates the RseA:sigmaE interaction in the cytoplasm and the availability of sigmaE RNA polymerase. J Biol Chem 275:33898–33904.
10. Kim DY, Jin KS, Kwon E, Ree M, Kim KK (2007) Crystal structure of RseB and a model of its binding mode to RseA. Proc Natl Acad Sci USA 104:8779–8784.
11. Jin KS, Kim DY, Rho Y, Le VB, Kwon E, Kim KK, Ree M (2008) Solution structures of RseA and its complex with RseB. J Synchrotron Radiat 15:219–222.
12. Wollmann P, Zeth K (2007) The structure of RseB: a sensor in periplasmic stress response of *E. coli*. J Mol Biol 372:927–941.
13. Ahuja N, Korkin D, Chaba R, Cezairliyan BO, Sauer RT, Kim KK, Gross CA (2009) Analyzing the interaction of RseA and RseB, the two negative regulators of the sigmaE envelope stress response, using a combined bioinformatic and experimental strategy. J Biol Chem 284:5403–5413.
14. Li X, Wang B, Feng L, Kang H, Qi Y, Wang J, Shi Y (2009) Cleavage of RseA by RseP requires a carboxyl-terminal hydrophobic amino acid following DegS cleavage. Proc Natl Acad Sci USA 106:14837–14842.
15. Otwinowski Z, Minor W (1997) Processing of X-ray diffraction data collected in oscillation mode. Methods Enzymol 276:307–326.
16. McCoy AJ, Grosse-Kunstleve RW, Adams PD, Winn MD, Storoni LC, Read RJ (2007) Phaser crystallographic software. J Appl Crystallogr 40:658–674.
17. Brunger AT, Adams PD, Clore GM, DeLano WL, Gros P, Grosse-Kunstleve RW, Jiang JS, Kuszewski J, Nilges M, Pannu NS, Read RJ, Rice LM, Simonson T, Warren GL (1998) Crystallography & NMR system: a new software suite for macromolecular structure determination. Acta Crystallogr D54:905–921.
18. Emsley P, Cowtan K (2004) Coot: model-building tools for molecular graphics. Acta Crystallogr D60:2126–2132.
19. Murshudov GN, Vagin AA, Dodson EJ (1997) Refinement of macromolecular structures by the maximum-likelihood method. Acta Crystallogr D53:240–255.
20. DeLano WL (2006) The PyMOL molecular graphics system. CA: DeLano Scientific LLC.
21. Reynolds C, Damerell D, Jones S (2009) Protorp: a protein-protein interaction analysis tool. Bioinformatics 25:413–414.